agriculturalengineering.eu 80(1), 2025, 104–124

DOI:10.15150/ae.2025.3332

agricultural
engineering.eu

Mapping of maize seeds by UAV as a test method for precision seeding technology under field conditions

Steffen Konnemann, Eike Hunze, Frank Beneke

This study presents three approaches to further develop the testing framework for precision planters in field operations, as applied by the German Agricultural Society (DLG), and derives a remote sensing-based methodology from it. By utilising a UAV equipped with an RGB sensor, we semi-automatically segmented and mapped maize seeds planted by a precision planter on reconsolidated soil. We achieved this by applying the Otsu threshold to the a*-scale of the CIELab colour space, followed by filtering for the area of a representative maize seed. The mean visibility rate for openly placed maize seeds was greater than 90%. The segmentation algorithm detected visible maize seeds with high recall of ≥ 96%, although the precision of ≥ 62% still requires further improvement. Double placements were detected with an equivalent error rate from a distance of two centimetres or more. The mapping of seed placement points, with an $RMSE_{xy}$ between 1.7 and 5.1 mm was more accurate than in comparable studies using plant-based mapping. The results of this study lay the foundation for adapting the DLG testing framework to the technical advancements in precision planting technology.

Keywords

Planters, Precision planters, Seeds, Drone, UAV, Spacing, Uniformity, Segmentation, CIELab

The achievable grain yield of maize (*Zea mays* L.) depends on the four yield factors: plant density, number of cobs per plant, number of kernels per cob, and kernel weight. (Assefa et al. 2016). Compared to tillering grass species, maize plants do not compensate for low plant densities by branching (Sangoi 2001). Conversely, high plant densities can lead to a decline in the yield per plant, attributable to increased competition for light, water, and nutrients (Duncan 1984, Sangoi 2001). Consequently, precision seeding technology has undergone continuous development over the past few decades, with the objective of exploiting the yield potential through the evenness of seed spacing and the uniformity of plant stands (Zhang et al. 2018).

The functions of a precision planter include opening a furrow, singulation and transportation of the seed to the furrow, as well as covering and firming the seed with soil (Panning et al. 2000). Possible metrics for planter performance that arise from this are the variability around the target drop point (intended position), the failure to place a seed (missed spot), and the simultaneous placement of multiple seeds (double placement) (Panning et al. 2000).

In order to facilitate a comparative evaluation of the performance factors of different precision planters, the standard ISO 7256-1:1984 was published in 1984 (International Organization for Standardization 1984). The current suite of test frameworks applied, including those developed by the American Society of Agricultural and Biological Engineers (Kachman and Smith 1995) and the

received 14 November 2024 | accepted 18 February 2025 | published 17 March 2025

German Agricultural Society (DLG) (Deutsche Landwirtschafts-Gesellschaft 1991), are grounded in this standard. The tests can be categorised into two distinct methods: laboratory tests and field tests. Laboratory tests are adequate for preliminary investigations, however, field testing is imperative to account for factors such as planter bounce and seed movement within the furrow (Panning et al. 2000, Budde 2016).

In the field test of precision planters conducted by the DLG, three maize varieties are planted at varying driving speeds on a pre-prepared seedbed. The field test is designed to evaluate the precision of seed placement, the distribution of seeds, and the field emergence of the plants. Two to four weeks after planting, the distances between four sets of 250 maize plants within a row per variant are measured using a mobile distance measuring device. The operator manually propels the distance measuring device along the plant row, and the recording button is subsequently activated to obtain measurements for plant-to-plant distances (Deutsche Landwirtschafts-Gesellschaft 1991, Schuchmann 2019).

The limitations of the established DLG testing methodology lie in (1) the exclusive measurement of plant-to-plant distances within a row, (2) the measurement is taken on only a small portion of the total area, and (3) the consideration of emerged maize plants, whose survival rate is affected by environmental factors.

(1) The optimization of plant spacing for maize through adjusted row widths and planting in equidistant spacing has gained importance in recent years (Griepentrog 1999, Götz und Bernhardt 2010, Schuchmann 2019). The underlying reasons for this phenomenon are manifold. In addition to yield advantages, environmental benefits are realised through faster shading of weeds and improved nutrient utilisation. Furthermore, an increase in the area that can be worked by hoeing is observed, from 66% to 90% (Hoff und Mederski 1960, Bullock et al. 1988, Götz und Bernhardt 2010). Whilst the calculation of the plant spacing distribution as an evaluation measure of equidistant planting can be performed by the measurement of the plant-to-plant distance within a row, this is only possible with a fixed row width and consistent planting density. The recording of the plant coordinates across multiple rows in a Geographic Information System (GIS) would expand the possibilities for evaluation (Griepentrog 1999).

(2) Other trends in recent years include varying the planting rate, for example, depending on soil fertility (Woli et al. 2014), automatic control of sections, and the evaluation of telemetry data (Schuchmann 2019). The evaluation of these techniques is only possible through machine tests on a larger area, whereas the current assessment techniques employed in field tests are limited to manually sampling plant-to-plant distances (Deutsche Landwirtschafts-Gesellschaft 1991, Griepentrog et al. 2005, Bozdoğan 2008). Manual sampling is a laborious and time-consuming process, and is also subject to human subjectivity (Vong et al. 2021, Pathak et al. 2022). Studies have shown that the use of remote sensing technology to capture plant coordinates can overcome these limitations (Shuai et al. 2019, Pathak et al. 2022).

(3) The evaluation of precision planters based on emerged plants is problematic due to the confounding of influences of seed germination and the effects of the planter's performance. (Panning et al. 2000, Thorp et al. 2007). The survival rate of plants is dependent on a variety of factors, including nutrients, water, planting depth, herbicide residues, weather extremes, diseases, and solar radiation (Pathak et al. 2022). Consequently, within the DLG field test framework, the proportions of double placements and missed spots in the field trial are recorded, but not evaluated (Schuchmann 2019).

It has been demonstrated by other field test frameworks that the direct measurement of the planted seeds can be an alternative. However, this method is time-consuming and there is a risk of altering the seed's placement position when opening the furrow (Panning et al. 2000).

The aforementioned limitations have given rise to a growing interest in recent years in the utilisation of remote sensing techniques for agricultural field trials (Pathak et al. 2022). Remote sensing is defined as the process of detecting and monitoring physical properties in a given space. In the agricultural context, for example, the reflected or emitted radiation of a field or a plant is captured from a distance using various platforms (National Aeronautics and Space Administration 2019). In the context of field trial research, unmanned aerial vehicles (UAVs) are predominantly utilised as a platform. They offer a flexible spatial and temporal resolution, a manageable data collection effort, and are more cost-effective than manned aircraft (Pathak et al. 2022). The utilisation of UAVs in plant segmentation and mapping has already been demonstrated in a variety of contexts, including the cultivation of cotton, potato, maize, fruit trees, rapeseed, sorghum, wheat, and sugarcane (Shuai et al. 2019, Pathak et al. 2022). The image processing in these studies ranges in complexity from simple image and colour processing using filter algorithms to multi-layered analyses using machine learning (Pathak et al. 2022). In the domain of image and colour processing, the employment of either special vegetation indices, which are calculated from individual reflection bands, or alternative colour spaces applied through a non-linear transformation of the RGB colour space is commonplace (García-Martínez et al. 2020). For instance, in their study, Zhang et al. (2018) proposed an extraction methodology for mapping maize plants utilising the Excess Green Index, subsequently followed by image segmentation using the Otsu threshold value (Otsu 1979). Utilising a combination of filters for the area and shape of representative maize plants, the background noise was filtered out and individual plants were connected. Information regarding the height and angle of the camera, in addition to the average height of the maize stand, was utilised to approximate the coordinates of the maize plants. Row detection, achieved through the use of information on driving direction and row spacing during planting, enabled the calculation of plant-to-plant distances within a maize row (Zhang et al. 2018). As demonstrated by Shuai et al. (2019), the methodology was applied in a field setting, resulting in a recall of > 0.95 and a precision of > 0.97 when counting 129 to 141 maize plants per row, with three repetitions per treatment. In the context of plant mapping, deviations ranging from 17 mm to 26 mm with an R^2 of 0.9 were observed. (Shuai et al. 2019). García-Martínez et al. (2020) utilised the a*-scale of the CIELab colour space (Commission Internationale de l'Eclairage 2007) with a threshold value of zero for the segmentation of maize plants, subsequently employing a filter through normalised cross-correlation. In the segmentation of maize plants within the field trial, a recall of > 0.90 was attained; however, no measurement of plant distances was conducted (García-Martínez et al. 2020). All studies concur that the measurement of plant coordinates is only possible with limitations. The time window in which individual maize plants can be adequately distinguished is very brief, as the growing plants increasingly overlap (Gnädinger and Schmidhalter 2017, García-Martínez et al. 2020, Pathak et al. 2022). Furthermore, the presence of weeds has been shown to have an impact on the segmentation process. This is due to the fact that weeds can reflect a similar colour spectrum to that of maize plants (Gnädinger and Schmidhalter 2017, Shuai et al. 2019, García-Martínez et al. 2020). Additional challenges emerge due to variations in solar radiation and an accumulation of plant residues on the soil surface (Golzarian et al. 2012).

The motivation for conducting this research work arises from the limitations of the DLG testing framework for precision planters in field operations, as well as the difficulties in remotely sensing plant coordinates via the plants themselves. The objective of the research is to develop a methodology for testing precision planters in field operations that utilizes UAVs as a remote sensing platform to map visibly planted maize seeds. From this objective, the following research questions arise:

(1) Is the visibility rate of maize seeds during precision planting with an open furrow comparable to the survival rate of maize plants?

(2) Is it possible to capture, segment, and determine the position of visibly planted maize seeds using a UAV?

The primary objective of research question (1) is to further develop the DLG field testing framework, with the aim of transitioning from the measurement of plants to the measurement of seeds (Figure 1). In a subsequent step, the objective of research question (2) is to develop a partially automated measurement methodology for the georeferenced mapping of seeds, with the intention of replacing manual distance measurement.

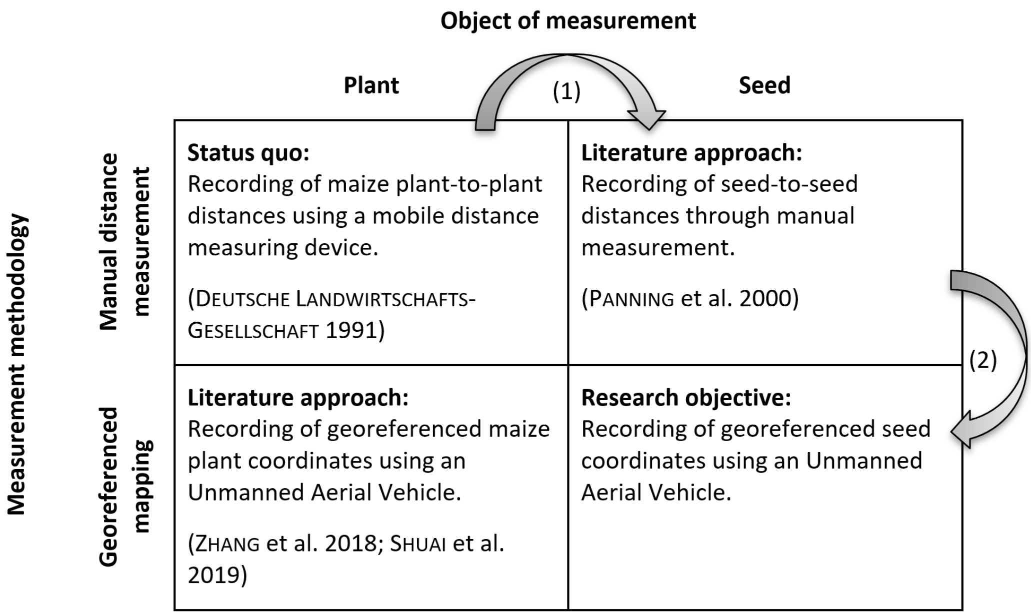

Figure 1: Graphical summary of the objectives and research questions

Material and Methods

Study Location and Preparatory Measures

The field trial was conducted in September 2023 on a field south of Göttingen (Germany, 51°29’42.8”N 9°56’05.8”E, WGS84). The Landesamt für Bergbau, Energie und Geologie Niedersachsen (2023) has classified the soil type of the field as a medium Chernozem-Parabraunerde, indicating a silty-clayey composition. The crop residues and the regrowth of the previous crop, winter rapeseed, were incorporated into the soil on two occasions, at an interval of 14 days, using a cultivator to a depth of 10 cm prior to the experiment. On the day of the experiment, a rotary harrow was used to ensure an even distribution of soil moisture and to incorporate the remaining organic matter to a depth of 15 cm at a 90° angle to the later experimental setup.

Preliminary trials demonstrated that reconsolidating the soil and fixing the pressure roller of the precision planter in a non-working position were suitable measures to visibly plant maize seeds in an open furrow. Therefore, a targeted reconsolidation of the soil was carried out in two-factor levels (high/low compaction) for the experiment. The high compaction level was achieved using the tyres of a Fendt 718 Vario (weight: 9,070 kg, front tyres: 540/65R30, rear tyres: 650/65R42) with a calculated average contact area pressure of 0.90 bar. Concurrently, a low compaction level was realised through the utilisation of an attached tyre roller equipped with Alliance Flotation 339 Matrix tyres (weight: 1,425 kg, tyres: 400/55R17.5), achieving a calculated average contact area pressure of 0.67 bar. A georeferenced wayline was loaded onto the tractor's RTK-GNSS steering system using the NEXT Farming Live software as of 23 September 2023 (FarmFacts GmbH, https://www.nextfarming.com/software/next-farming-live-1/) for driving on the test site. The track spacing was 4.5 m. Each of the 55 m long experimental strips was driven over six times at a speed of 5 km/h. The compaction success was documented with the help of the Penetrologger 06.15.SA (v6.03; Royal Eijkelkamp, NL) at five measurement points per track in the middle of the experimental setup. As illustrated in Figure 2, the cone penetration resistance was measured over the first 15 cm. Concurrently, the soil moisture content was determined by taking and drying soil samples from the top six centimetres. The mean value recorded was 14.6%, with a standard deviation of 0.3%.

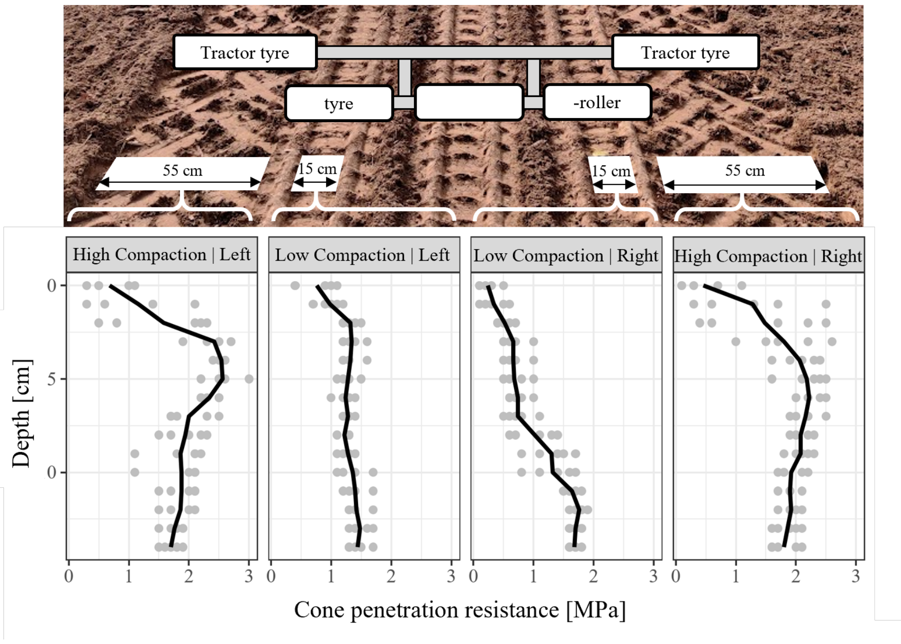

Figure 2: Top: Photographic representation of the reconsolidated soil with a sketch that illustrates the arrangement of tractor tyres and tyre rollers (the dimensions indicate the width of the reconsolidated track, into which the units of the precision planter subsequently worked); bottom: the cone penetration resistance measured per row in the center of the experiment, depending on the depth (the black line represents the mean value; the data was collected at a mean water content of 14.6%)

Manual and Precision Planting of Maize Seeds

The target object for detection was conventional maize seed with a reddish, fungicidal coating. The thousand-seed weight of the batch used was 283 grams.

To develop a segmentation algorithm for maize seeds that is also robust against double placements, 0.5 x 5 m test plots were established in the northern part of the field trial by manually planting seeds (Figure 3). In order to achieve the greatest possible similarity to the maize seeds planted by the precision planter, the test plots were previously reconsolidated to the same extent and driven over by the precision planter at a speed of 8 km/h. The maize seeds were then manually planted in the four-factor levels: single seed, 0 cm distance, 1 cm distance, and 2 cm distance, using a self-constructed planting aid (Figure 3). The planting was conducted in three blocks, with five repetitions per planter unit position for each factor level.

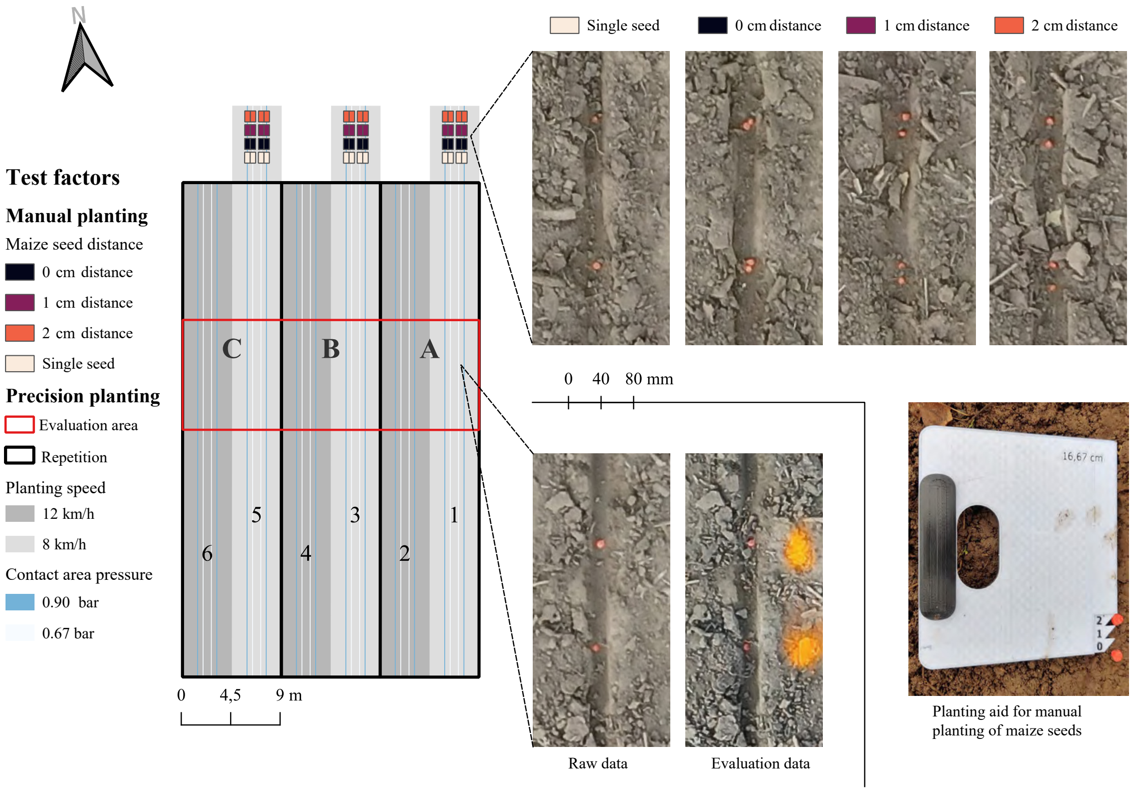

Figure 3: Overview of the experimental setup (North: Manual planting of maize seeds with a specially constructed planting aid at predefined distances in furrows formed by the precision planter; South: Precision planting at 8 km/h and 12 km/h in soil reconsolidated with 0.67 bar and 0.90 bar, respectively; the numbering indicates the pass of the precision planter and the lighting scenario during the UAV flight; the images depict excerpts from the orthomosaics of the first UAV flight for raw data collection; in the red-framed evaluation area, a second UAV flight was conducted to document the manual marking of the maize seeds with spray paint, visible in the second image at the bottom right)

In order to ascertain the viability of precision planting of maize seed with an open furrow, and to evaluate the performance of the developed segmentation algorithm, maize seeds were planted using a precision planter in the previously reconsolidated strips. The experimental setup comprised a Fendt 314 Vario and the Precea 4500-2CC Super from Amazonen-Werke H. Dreyer SE & Co. KG. The experimental strips were traversed using an RTK-GNSS steering system and the wayline from the previous reconsolidation measure. The passes were conducted at two-factor levels: 8 and 12 km/h, from south to north. In accordance with the precision planters operating instructions, singulation discs with a 5 mm bore were utilised, the fan drive was programmed to 45 mbar, and the seed shutter was set to position F. The positions of the four middle planter units of the six-row precision planter employed were adjusted to the track width of the compacted rows. The pressure rollers were fixed in a non-working position to prevent the closure of the furrows with soil. After two trial runs on test strips adjacent to the trial strips, the depth setting D was selected for the planting units in the high compaction level and the depth setting B for the planting units in the low compaction level. The decision was based on a qualitative evaluation between a too shallow furrow with an increased risk of rolled-out maize seeds and a too deep furrow with an increased risk of buried maize seeds. The furrows in the experiment had a depth of approximately 1 cm and a width of approximately 2 cm. The target distance for seed singulation was set to a common practice of 16.67 cm.

Collection of Raw and Evaluation Data Using a UAV

For data collection, a DJI Matrice 300 RTK quadcopter and a Zenmuse P1 RGB sensor with a 50 mm lens were used (DJI Technology, China). Flight planning was carried out in DJI Pilot 2 based on the georeferenced experimental design. To ensure the detection of the maize seeds, the flight altitude was set to 12 m above the starting point, resulting in a ground sampling distance (GSD) of 1 mm/px. Preliminary tests showed that an expected number of 25 pixels fully covered with maize seeds could be attained, which is above the minimum of four pixels per object to be detected as outlined in the literature (Hengl 2006). The experimental area was mapped with a lateral overlap of 70% and a longitudinal overlap of 80% between the images.

The first UAV flight for the collection of raw data was conducted immediately after the planting of maize seeds on 19 September 2023, between 15:48 and 16:14 local time, in changing cloudy weather conditions. The trajectory of the flight was oriented parallel to the experimental plots along the north-south axis of the experimental setup. This allows for the later analysis of potential weather influences on the segmentation outcome by breaking down the experimental plots into lighting scenarios. After spray painting all planted maize seeds in the 10-metre-long evaluation area, the second UAV flight took place between 16:48 and 17:04 local time, in changing cloudy weather conditions, for the digital documentation of the on-ground evaluation (Figure 3). The flight trajectory of this second flight route was perpendicular to the first.

The processing of the individual images followed the standard procedure for creating an orthomosaic in Agisoft Metashape (v1.7.2; Agisoft LLC, https://www.agisoft.com). First, we aligned the images using accuracy = high and real-time kinematic (RTK) of the UAV as a reference. The second orthomosaic was georeferenced to the first orthomosaic using the coordinates of the laid-out ground control points. This allowed for the later allocation of raw data and manual evaluation. The creation of the dense point clouds was done with quality = high and depth filtering = mild. The digital elevation models generated from the dense point clouds had a ground resolution of 2 mm/px each. Consequently, the two created orthomosaics were exported for further processing as GeoTiff with a ground sampling distance of 1 mm/px.

Descriptive Analysis of the Visibility Rate of Mechanically Planted Maize Seeds

The response to research question (1), which pertains to the comparison of the visibility rate of maize seeds with an open furrow and the survival rate of maize plants, is presented in a descriptive manner in this study. The test criterion is the visibility rate of maize seeds per row within a 10-metre-long evaluation zone situated within the 55-metre-long experimental strips (Figure 3). In this zone, between 48 and 59 maize seeds per row were planted by the precision planter, which corresponds to average distances between the maize seeds of 20.83 to 16.95 cm. The visibility rate of the maize seeds is calculated as the total number of all planted maize seeds minus the maize seeds that rolled out of the furrow and the maize seeds that were buried by soil due to the collapse of the furrow, in relation to the total number of all planted maize seeds (Equation 1):

$$visibility\ rate = \frac{all\ maize\ seeds - rolled\ out - buried\ by\ soil}{all\ maize\ seeds} \quad \text{(Eq. 1)}$$

The total number of maize seeds and the number of rolled-out maize seeds per experimental strip could be manually counted in QGIS-3.28.4 based on the colour markings in the orthomosaic of the second UAV flight (QGIS Association, https://www.qgis.org). As a reference count for determining the buried maize seeds, the orthomosaic of the raw data collection was visualized in QGIS at a scale of 1:2, and the center of the visible maize seeds was manually documented in a point layer in vector data format and subsequently counted. The descriptive analysis of the number of rolled-out, buried, and visible seeds per experimental unit was performed in R-4.3.2 (R Core Team, https://www.r-project.org). A target value of 90% was set for the visibility rate of the maize seeds, which corresponds to the legally established minimum germination capacity of maize seeds sold on the market (Anlage 3 SaatV). In field trials, field emergence rates between 86% and 96% have been observed (Nielsen 1993, Voit et al. 2010, Bouten et al. 2019).

Development of a Segmentation Algorithm for Maize Seeds

Pre-processing of Image Color into the CIELab Color Space

The images captured by the UAV were in the RGB colour space. In order to achieve robust segmentation performance in outdoor environments, independence from changing illumination intensities and a high contrast between the background and the target object were necessary (Golzarian et al. 2012, Gnädinger and Schmidhalter 2017, Mardanisamani and Eramian 2022). In the 8-bit RGB model, each pixel consists of three values between 0 and 255 for the colour components red (R), green (G), and blue (B). However, the high sensitivity of the RGB model to illumination has been shown to compromise its performance in outdoor environments (Golzarian et al. 2012, Riehle et al. 2020).

A colour space frequently used successfully for the purpose of robust segmentation of crops is CIELab (García-Martínez et al. 2020, Riehle et al. 2020, Pathak et al. 2022). This colour space was developed by the Commission Internationale de l'éclairage (CIE) for industrial purposes to represent colour in a way that is comparable to human perception (Hernández-Hernández et al. 2016). The ability of this colour space to isolate the lightness in a scale that is independent of the colour values enables segmentation that is more resistant to illumination fluctuations (Riehle et al. 2020). Through the non-linear transformation of the RGB colour space, the two chromatic scales a* and b* can be generated. The a*-scale represents the colour gradient from red to green, and the b*-scale represents the colour gradient from yellow to blue (Hernández-Hernández et al. 2016, García-Martínez et al. 2020). For the conversion of the RGB colour space to the CIELab colour space, a transformation to the CIEXYZ colour space (Commission internationale de l'eclairage 2007) was first performed using Equation 2:

$$\begin{bmatrix} X \\ Y \\ Z \end{bmatrix} = \begin{bmatrix} 0.490 & 0.310 & 0.200 \\ 0.177 & 0.813 & 0.011 \\ 0.000 & 0.010 & 0.990 \end{bmatrix} \begin{bmatrix} R \\ G \\ B \end{bmatrix} \tag{Eq. 2}$$

The lightness L* was transformed from the CIEXYZ colour space using Equation 3:

$$L^* = \begin{cases} 116\left(\frac{Y}{Y_n}\right)^{\frac{1}{3}} - 16, & for\ \frac{Y}{Y_n} > 0.008856 \\ 903.3\left(\frac{Y}{Y_n}\right)^{\frac{1}{3}} & for\ \frac{Y}{Y_n} < 0.008856 \end{cases} \tag{Eq. 3}$$

the a*-scale and the b*-scale were obtained from Equations (4) and (5):

$$a^* = 500\left[f\left(\frac{X}{X_n}\right) - f\left(\frac{Y}{Y_n}\right)\right] \tag{Eq. 4}$$

$$b^* = 200\left[f\left(\frac{Y}{Y_n}\right) - f\left(\frac{Z}{Z_n}\right)\right] \tag{Eq. 5}$$

where:

$$\begin{aligned} f(t) &= t^{\frac{1}{3}} & for\ t > 0.008856 \\ f(t) &= 7.787t + \frac{16}{116} & for\ t < 0.008856 \end{aligned} \tag{Eq. 6}$$

The variables X_n, Y_n and Z_n are determined by the white light colour used. In this study, D65, representative of indirect daylight, was chosen (Commission internationale de l'eclairage 2007). The transformation was applied to the orthomosaic of the raw data collection using the *convertColor()* function of the R package grDevices (v4.4.1; R Core Team). Preliminary investigations showed that the a*-scale is particularly well suited for detecting maize seeds. The a*-scale is largely independent of lightness, with green plant residues being automatically removed by excluding negative values. Furthermore, the conventional coating of the used maize seeds distinguishes itself from the soil in the red colour range. Figure 4 illustrates this by comparing the individual bands of the RGB and CIELab colour spaces for two randomly selected excerpts from the precision planted test plots. In this comparison, an excerpt with direct sunlight is explicitly contrasted with an excerpt with cloudy weather.

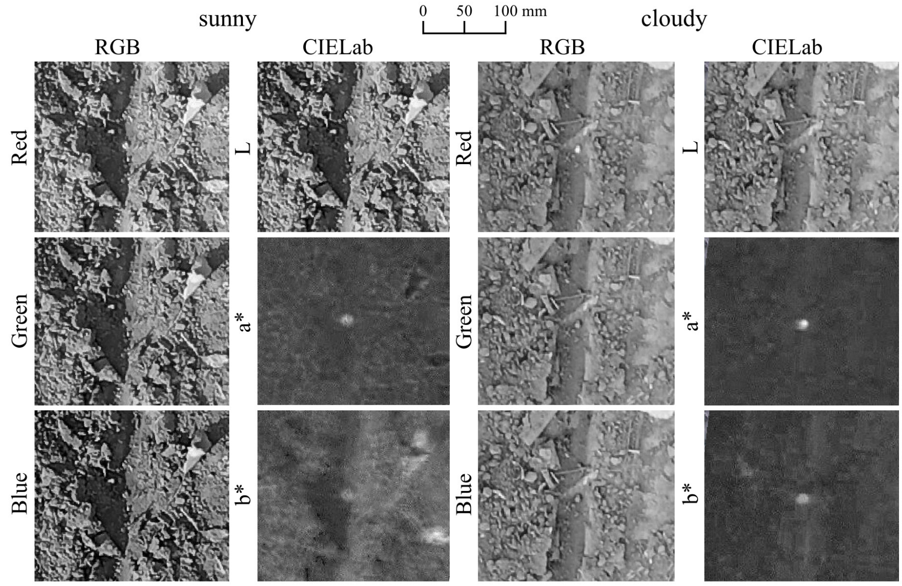

Figure 4: Comparison of RGB and CIELab color spaces for two randomly selected excerpts from the precision planted test plots, differentiated by images taken in sunny and cloudy weather conditions; Note: Representation of own data in accordance with Midtiby and Pastucha (2022)

Image Processing

The objective of image processing was to attain a reliable classification of maize seeds and soil through the following three stages:

(1) The minimisation of superfluous data and noise.

(2) The application of a semi-automatic thresholding method for a coarse pre-classification with high sensitivity, without the necessity for training data.

(3) The application of a simple post-processing procedure to optimise the classification performance.

(1) Minimisation of superfluous data and noise: The foundation for minimising the amount of data entering the analysis was the GIS-based experimental design and the implementation of an RTK-GNSS steering system during the experimental setup. By leveraging the information regarding the position of the planter units relative to the tractor centre, the planted experimental strips could be cut to a width of eight centimetres per planter unit. The R packages sf (v1.0.17; Pebesma, https://doi.org/10.32614/CRAN.package.sf) and terra (v1.7.78; Hijmans, https://doi.org/10.32614/CRAN.package.terra) were utilised for this purpose.

(2) Semi-automatic thresholding method: In the subsequent stage, the transformation of the RGB colour space to the CIELab colour space was conducted, as delineated in the preceding chapter. Negative pixel values in the employed a*-scale are indicative of green biomass and were excluded from the analysis through the removal of negative values. Conversion of the positive pixel values to the integer data format was achieved by multiplying by 1,000,000 and rounding to whole numbers. A threshold for two classes was then calculated using the Otsu algorithm (Otsu 1979), implemented within the R package autothresholdr (v1.4.2; Landini et al. 2017, https://doi.org/10.32614/CRAN.package.autothresholdr). The a*-scale values and the Otsu threshold were then converted back to their original format by dividing by 1,000,000. Pixel values above the threshold corresponded to the predicted pixels for maize seeds, and pixel values below the threshold were classified as soil. Due to potentially

changing lighting conditions during the UAV flight, a separate Otsu threshold was calculated and applied for each pass of the precision planter.

(3) Optimisation of the classification performance: As demonstrated in related studies, the number of false positive (FP) and false negative (FN) classified pixels can fluctuate due to the low proportion of maize seed pixels in relation to the total number of pixels, the presence of a crumbly soil surface, and the variation in lighting quality (Zhang et al. 2018, Midtiby and Pastucha 2022). To enhance the classification performance, a filter was implemented as a post-processing step to the binary orthomosaic, with the threshold value for the minimum number of connected pixels in four directions for the maize seed class serving as the basis. All groups classified as maize seeds with a number less than the threshold value were assigned to the soil class. The threshold value can be approximated manually by iterative testing and qualitative evaluation of the results. The number of pixels per maize seed, which can be derived from the used GSD and the area of a representative maize seed, serves as a guideline. In this study, the threshold value estimation was performed by minimizing false positive (FP) and false negative (FN) classified maize seeds in the manually planted test plots for segmentation testing. Finally, by calculating the centroid of each pixel group of the maize seed class, a conversion from the raster format to the vector format was performed. This file was then used to calculate the number of segmented maize seeds and to analyse their mapped positions.

Evaluation of the Segmentation Performance of the Algorithm

The performance of the algorithm in detecting maize seeds was evaluated by comparing it with the digital manual count of visible maize seeds. The evaluation process involved planting the evaluated seeds through six passes, with four rows each. The orientation of the UAV flight trajectory was parallel, which enabled the analysis of the effects of lighting fluctuations due to changing weather conditions. Therefore, each pass was considered as a lighting scenario in the evaluation.

The evaluation process involved the calculation of precision (the proportion of correctly identified maize seeds out of all recognised maize seeds) and recall (the proportion of correctly identified maize seeds out of all maize seeds). These metrics were derived using Equations 7 and 8:

$$precision = \frac{TP}{TP + FP} \qquad \text{(Eq. 7)}$$

$$recall = \frac{TP}{TP + FN} \qquad \text{(Eq. 8)}$$

with TP, FP, and FN representing the number of true positives, false positives, and false negatives, respectively. The F1-Score was utilised as the weighted average of precision and recall for the joint consideration of the two evaluation parameters, as per Equation 9 (Csurka et al. 2013):

$$F1 - score = \frac{2 \times precision \times recall}{precision + recall} \qquad \text{(Gl. 9)}$$

Evaluation of the Mapping Performance of the Algorithm

The performance of the algorithm in terms of mapping maize seeds was evaluated by comparing it with the digital manual mapping of the centre of the maize seeds through visual interpretation of the raw data orthomosaic. For the evaluation, the root mean square errors (RMSE) for Easting (X direction), Northing (Y direction) and radial direction (XY direction) of the coordinates from the UTM32 coordinate reference system in millimetres was calculated using Equations 10, 11 and 12:

$$RMSE_x[mm] = \sqrt{\frac{1}{n}\sum_{i=1}^{n}\left(x_{i(pred)} - x_{i(obs)}\right)^2} \times 1000, \quad \text{(Eq. 10)}$$

$$RMSE_y[mm] = \sqrt{\frac{1}{n}\sum_{i=1}^{n}\left(y_{i(pred)} - y_{i(obs)}\right)^2} \times 1000, \quad \text{(Eq. 11)}$$

$$RMSE_{xy}[mm] = \sqrt{RMSE_x{}^2 + RMSE_y{}^2}, \quad \text{(Eq. 12)}$$

where

$x_{i(pred)}$ and $y_{i(pred)}$ are the coordinates for Easting and Northing of the i^{ten} predicted maize seed, respectively,

$x_{i(obs)}$ und $y_{i(obs)}$ are the coordinates for Easting and Northing of the i^{ten} observed maize seed, respectively,

n is the number of maize seeds tested, and

i is an integer ranging from 1 to n (ASPRS Map Accuracy Standards Working Group 2015).

The evaluation methodology is considered valid under the assumption that the distribution of individual residuals is similar to a normal distribution and the average error value is relatively small compared to the target accuracy (ASPRS Map Accuracy Standards Working Group 2015). With regard to the target value for horizontal accuracy, this study aimed for twice the GSD, which is two millimetres.

Results and Discussion

In order to maintain the thematic context, the results obtained are discussed directly. Firstly, the influence of the test factors – namely planting speed, reconsolidation, and repetition – on the visibility rate of maize seeds during mechanical planting is reported. Subsequently, the results of the semi-automatic segmentation and mapping of maize seeds are analysed and discussed.

Visibility Rate of Maize Seeds during Precision Planting

In 13 out of the 24 experimental rows, no rolling of maize seeds out of the furrow was observed. In eight cases, one maize seed rolled out, and in three cases, two maize seeds rolled out (Figure 5). This indicates that the proportion of non-rolled seeds ranges between 96% and 100%. Upon visual examination, no discernible pattern emerges with respect to the influence of the test factors, namely planting speed, reconsolidation, and repetition.

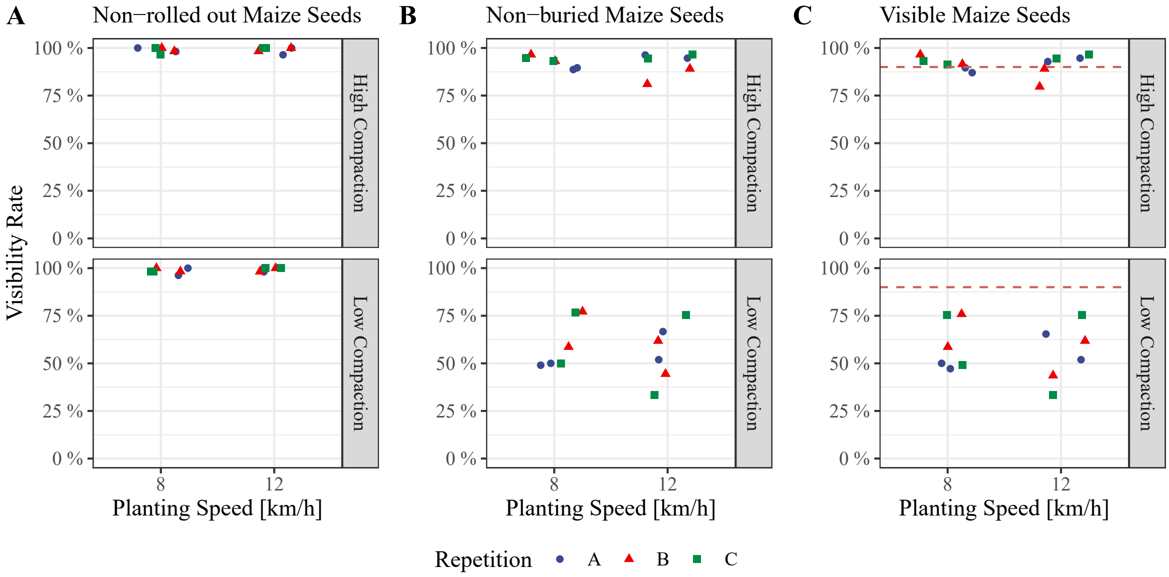

Figure 5: Proportion of non-rolled out (A), non-buried (B), and therefore visible maize seeds (C) as a function of planting speed, faceted by compaction level (a random horizontal shift of the points was added to differentiate between points with the same value; the dashed line marks the target of a visibility rate of ≥ 90%)

In relation to the burial of maize seeds in soil, a clear distinction emerges with respect to soil compaction. At high levels of compaction, visibility rates ranging from 81 to 97% are observed, while at low levels of compaction, the visibility rates are lower, ranging from 33 to 77%. With regard to the test factor of planting speed, no discernible pattern is evident at high levels of compaction. However, at low compaction levels, a decline in visibility, accompanied by an increase in dispersion, was observed when the planting speed was elevated from 8 to 12 km/h.

The visibility rate of maize seeds, as a combined measure of rolled out and buried seeds, shows no deviating observations. The defined target visibility rate of 90% is not achieved in any case at low compaction. At high compaction, the target is not achieved in four out of twelve rows. The remaining eight visibility rates, ranging from 91 to 97%, are within the desired target range.

From the descriptive analysis of the rate of visible maize seed placement by a precision planter in this field trial, three conclusions can be drawn:

(1) Only a negligible proportion of maize seeds rolled out from the 8-centimetre-wide area of the digitally captured furrow. Consequently, rolling had only a minor influence on the final visibility rate compared to burial. Rolling of maize seeds within the furrow after leaving the seed tube could not be evaluated. However, as described by Panning et al. (2000) the functions of precision planters also include covering the seed with soil. The rolling of maize seeds in the furrow is influenced by soil conditions and driving speed in this process (Panning et al. 2000). Given the alterations to the soil conditions caused by the reconsolidation process in this trial, further investigation is necessary to ascertain the extent to which rolling in the row influences the final position of the maize seeds.

(2) In relation to the velocity of the precision planter, it was initially assumed that the rate of visibly planted seeds would decrease with increasing speed. However, the descriptive analysis revealed this to be only observable at low compaction levels. A subsequent study utilising a more extensive dataset at higher driving speeds is required to further ascertain the independence of the methodology employed from the driving speed of the precision planter.

(3) The objective of achieving a visibility rate of ≥ 90% for maize seeds, as established by the requisite germination capacity for approval and the emergence rates observed in field trials, was successfully met in eight out of twelve measurement rows under conditions of high compaction. The discrepancy in the four additional samples was negligible. Therefore, the visible planting of maize seeds in an open furrow with digital recording by UAV, and manual counting in a geographic information system, can be considered just as reliable as the currently applied method of counting emerged maize plants. To establish this methodology as a basis for a testing framework for precision planters, the objective of optimising soil conditions and reconsolidation measures to further enhance the visibility rate of maize seeds should be pursued.

Performance of Automatic Maize Seed Segmentation

The developed segmentation algorithm for maize seeds was applied to both the manually planted test plots with double placements and the precision planted strip trial. The former served to gain insight into which threshold value for the pixel filter leads to sufficient filtering of false positively (FP) recognised maize seeds, without actually present maize seeds being falsely classified as negative (FN). Additionally, the robustness in differentiating double placements was verified.

In the test plots with single maize seeds, as expected, the number of false negatives increased with the increase in the threshold value, while the number of false positives decreased (Figure 6). In the case of double placements, an enhancement in segmentation performance was evident with increasing distance between the maize seeds. Maize seeds positioned in close proximity (0 cm distance) were classified as single maize seeds across all threshold values, resulting in a static number of false negatives of 60. At a distance of two centimetres or more, the number of false negatives was comparable to that of single maize seeds. At low threshold values, an increased number of false positives was observed in all variants. The decrease in false positives to zero with an increase in the filter threshold value confirms the filter's ability to remove artefacts from the binary raster. For single maize seeds and at distances of two centimetres or more, the minimum number of error values was achieved with filter threshold values between 80 and 100, with a minimum at 90. Consequently, a filter threshold value of 90 was utilised for the application of the algorithm to the precision planted strip trial.

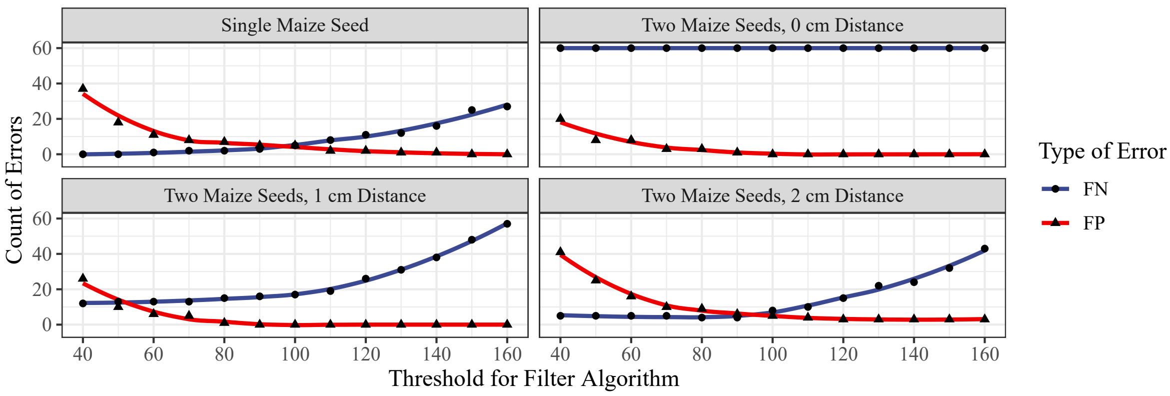

Figure 6: The validation results of the maize seed segmentation in the manually created test plots as a function of the threshold value for the filter algorithm, faceted by the four-factor levels to check the applicability to double placements

Table 1 illustrates the validation results of the segmentation algorithm when applied to the precision planted experimental strips with high compaction. Only in these strips an acceptable visibility rate of ≥ 90% was achieved, as described in the previous chapter. The digital manual enumeration of the visibly planted maize seeds served as a reference for the validation process. The validation results differed significantly depending on the prevailing lighting conditions during the UAV flight. The most unfavourable results were obtained in lighting scenarios 1 and 4. Visual inspection of the orthomosaic showed that during the flight at these times direct sunlight was present, as also evidenced by the highest mean values and standard deviations for the a*-scale. The Otsu threshold values were also the highest, at 3.60 and 3.92. The number of false positive maize seeds was considerably increased, resulting in very low precision. In lighting scenario 1, 61% of the maize seeds were not detected, and the recall was the lowest across all scenarios, at 0.39, resulting in a very low F1-score of 0.11. In the other scenarios 6, 2, 3, and 5, recall was very high, with values ≥ 0.96, due to the small number of undetected maize seeds. Lighting scenarios 3 and 5 had moderate precision of 0.67 and 0.62, respectively, due to an increased number of pixels falsely classified as maize seeds. This resulted in moderate F1-scores of 0.68 and 0.62, correspondingly. Scenarios 2 and 6, characterised by uniform cloud cover during data acquisition, had very high F1-scores of ≥ 0.95.

Table 1: Validation results for maize seed segmentation at high compaction per lighting scenario, sorted by descending F1-score.

Scenario	a*-scale		Otsu	TP[3]	FP[3]	FN[3]	Recall	Precision	F1-score
	M[1]	SD[2]							
6	1.57	1.90	2.68	111	3	0	1.00	0.97	0.99
2	1.67	2.27	3.48	107	10	1	0.99	0.91	0.95
3	1.78	2.15	3.25	110	54	2	0.98	0.67	0.80
5	1.69	2.20	3.30	105	64	4	0.96	0.62	0.76
4	2.25	2.43	3.92	83	212	15	0.85	0.28	0.42
1	2.23	2.31	3.60	35	494	55	0.39	0.07	0.11

[1] M = arithmetic mean
[2] SD = standard deviation
[3] TP = true positive, FP = false positive, FN = false negative

In summary, it can be posited that the developed methodology possesses the capacity to semi-automatically segment maize seeds, thereby facilitating the otherwise manual evaluation process (Vong et al. 2021, Pathak et al. 2022). The frequent challenges encountered in semi-automatic plant segmentation, such as plant residues or weeds, as well as the overlap of plant parts, are not encountered in the presented methodology (Golzarian et al. 2012, Gnädinger and Schmidhalter 2017, García-Martínez et al. 2020, Pathak et al. 2022). This is achieved by directly recording the maize seeds after the setup of the experiment, thereby ensuring that weeds have no opportunity to germinate. Additionally, the use of positive values of the a*-scale of the CIELab colour space automatically excludes all green plant components from the evaluation process.

The performance outcomes of scenarios 1 and 4, which yielded F1-scores of no greater than 0.42, can be considered substandard. This substandard performance, despite the implementation of an Otsu threshold calculation for each scenario, can be attributed to the presence of sunlight during the data acquisition process. This finding indicates that, despite the extraction of lightness in the

L*-scale of the CIELab colour space, a residual light component exerts an influence on the a*-scale. This results in a reduction in the disparity between the pixel values assigned to the maize seed and soil classes This condition is considered to be one of the limitations of the Otsu algorithm, as evidenced by Wang et al. (2020). Furthermore, a unimodal distribution of the a*-scale was observed in all lighting scenarios, which can be attributed to the relatively small proportion of maize seed pixels in comparison to soil pixels. This is a further challenge for thresholding with the Otsu algorithm, which was designed for bimodal distributions (Otsu 1979). The advancements of the Otsu algorithm, as described by Wang et al. (2020), have the potential to enhance the accuracy of the methodology when confronted with variable weather conditions. This should be investigated as an alternative. Furthermore, fundamentally different thresholding methods could be utilised and evaluated using the R package autothresholdr (Landini et al. 2017). Future studies should continue to focus on reducing the proportion of soil pixels entering the segmentation by using georeferenced experimental design, setting up the experiment with RTK-GNSS steering systems, and subsequently cropping the orthomosaic to the planting rows.

Performance of Semi-Automatic Maize Seed Mapping

The performance of the algorithm in terms of its ability to predict the georeferenced position of maize seeds was evaluated by the test parameters $RMSE_x$, $RMSE_y$, and $RMSE_{xy}$. The validity of applying these test parameters was verified by examining the residuals between the predicted and digitally evaluated maize seed coordinates for each lighting scenario (Figure 7). It could be observed that the distribution in all scenarios, with the exception of scenarios 1 and 4, resemble a normal distribution. The residuals for Easting in scenario 1 were characterised by a high degree of dispersion, resulting in a flat distribution. The median error for scenario 1 was shifted −1.44 mm westward for Easting and +1.58 mm northward for Northing. The median errors for the other lighting scenarios were found to be within the range of −0.61 and +0.01 mm for Easting and −0.37 and +0.34 mm for Northing. This indicates that all mean errors fell within the specified target accuracy of two millimetres, thereby validating the test parameters (ASPRS Map Accuracy Standards Working Group 2015).

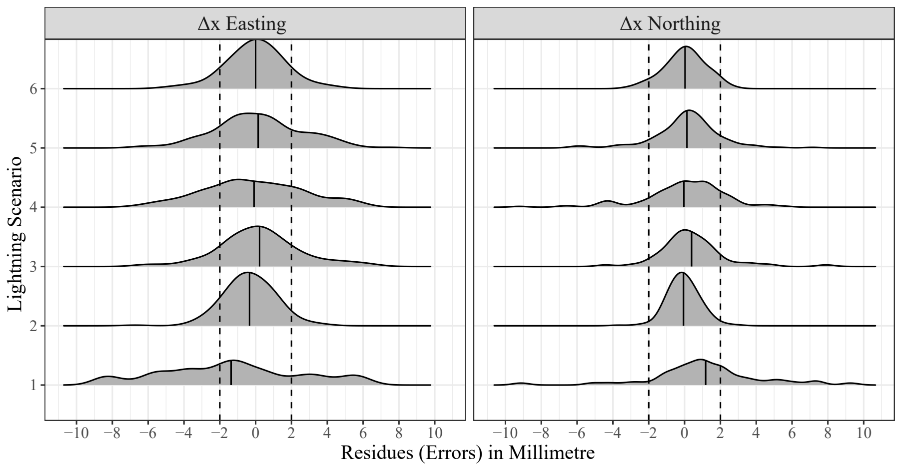

Figure 7: The distributions of the residuals of the predicted maize seed coordinates compared to the maize seed coordinates from the digital manual evaluation for each lighting scenario (the dashed lines mark the specified target accuracy of two millimetres, the solid line shows the mean error of each distribution)

The performance of the developed algorithm in terms of mapping is reported in Table 2 through the horizontal root mean square errors (RMSE) for Easting and Northing. It is evident from the data that the worst horizontal mapping accuracy was achieved in scenario 1, with an $RMSE_{xy}$ of 5.05 mm. This is attributable to the maximum error observed for Easting ($RMSE_x$ = 3.96 mm) and the maximum error observed for Northing ($RMSE_y$ = 3.12 mm) when compared to all scenarios. Conversely, the best horizontal mapping accuracy was achieved in scenario 2 with an $RMSE_{xy}$ of 1.72 mm. It is noteworthy that this scenario is the only one that falls within the specified target accuracy of two millimetres. Scenarios 6, 3, 5, and 4 exhibited $RMSE_{xy}$ values of 2.03 mm, 2.60 mm, 3.08 mm, and 3.60 mm, respectively. Therefore, they exceeded the specified target accuracy range but were below the maximum error observed for Easting ($RMSE_x$ = 3.96 mm) and Northing ($RMSE_y$ = 3.12 mm) by more than 1.45 mm. Across all lighting scenarios, it was observed that the root mean square error for Easting ($RMSE_x$) was 0.54 mm higher on average than the root mean square error for Northing ($RMSE_y$), with a standard deviation of 0.19 mm.

Table 2: Validation results for maize seed mapping per lighting scenario, sorted by ascending $RMSE_{xy}$ in mm

Scenario	**$RMSE_x$ [1)] in mm**	**$RMSE_y$ [2)] in mm**	**$RMSE_{xy}$ [3)] in mm**
2	1.43	0.95	1.72
6	1.68	1.13	2.03
3	2.01	1.65	2.60
5	2.49	1.82	3.08
4	2.71	2.36	3.60
1	3.96	3.12	5.05

[1)] $RMSE_x$ = the horizontal linear root mean square error in the X direction (Easting)
[2)] $RMSE_y$ = the horizontal linear root mean square error in the Y direction (Northing)
[3)] $RMSE_{xy}$ = the horizontal linear root mean square error in the radial direction that includes both X- and Y-coordinate errors.

As demonstrated in the previous chapter, two lighting scenarios examined in this study (i.e. 1 and 4) exhibited suboptimal performance in terms of maize seed segmentation. This finding is also evident in the mapping of maize seeds. The results suggest that strong lighting during data acquisition with the UAV negatively impacts the accurate mapping of maize seeds. This phenomenon can be attributed to the increased reflectance of the reddish maize seeds under direct sunlight, which leads to an increase in the a*-scale of the surrounding pixels. This results in an increase in the number of segmented pixels per seed, consequently leading to a less accurate mapping of the seed centre.

The higher residuals observed for Easting in comparison to Northing across all lighting scenarios can be explained by the reflectance of the maize seed environment. Due to the experimental setup being aligned along Northing, the seed furrow of the maize seed is level along the north axis. This results in a smaller number of soil pixels reflecting the reddish reflectance of the maize seed, due to the flat soil structure in the north-south direction. Conversely, on the east axis, the walls of the seed furrow are situated, thereby providing a more extensive reflective surface area. Consequently, the segmented maize seed pixel groups are oval in shape, extending in the east-west direction. This, in turn, results in increased inaccuracy when calculating the centroids along the east axis.

Notwithstanding the two aforementioned limitations, the applied methodology is well suited to the semi-automatic mapping of maize seeds. Although the specified target accuracy of two millimetres (twice the GSD) was only achieved in one scenario, the errors are negligible when compared to the semi-automatic mapping via the detection of maize plants. For instance, Shuai et al. (2019) attained an $RMSE_{xy}$ ranging from 17 to 26 mm when determining plant coordinates through the segmentation of maize plants, utilising the method developed by Zhang et al. (2018). Assuming the maximum possible error in mapping two maize seeds in this study to be 5.05 mm, a maximum error of 10.1 mm (= 2 × max($RMSE_{xy}$) = 2 × 5 mm) is obtained when checking the distance between the maize seeds. In contrast, the mapping method of Shuai et al. (2019) has a maximum error of 52 mm (= 2 × max($RMSE_{xy}$) = 2 × 26 mm). Zhang et al. (2018) also only achieved accuracies of around 30 mm during method development when calculating distances. According to the authors, the main reason for this is the assumption of a mean height for the maize plants, which is necessary for calculating the point of emergence of the plant from the soil. Consequently, for the accurate recording of the maize seed coordinates to assess the planting accuracy of a precision planter, direct mapping of maize seeds is preferable to indirect mapping via the calculation of the maize plant centre. The potential extension of this methodology to crops with smaller and differently coloured seeds, such as sugar beets or rapeseed, should be a focus of future research.

Conclusions

The planting of maize with a precision planter has become an important technical factor for optimising yields. The continuous development of precision planting technology also poses a challenge for the further development of current testing frameworks. In relation to the testing framework for precision planters employed in field operations by the DLG in Germany, three distinct approaches were identified: (1) The testing framework can be further developed from measuring distances within a row to a georeferenced recording of the plant coordinates. This facilitates expanded evaluation prospects beyond individual rows, enabling an objective assessment of the plant spacing distribution in its entirety, for instance, in equidistant planting. (2) Remote sensing techniques, such as sensors carried by a UAV, offer the possibility of transitioning from a random sample-based evaluation to a scalable measurement method with georeferencing. This also enables the testing of new technological advancements in precision planting, such as varying the seeding rate, automatic section control, and the evaluation of telemetry data accuracy. (3) The singulation performance of a precision planter in field operations can be made more transparent by considering the planted seeds instead of the emerged plants, allowing for a clearer distinction from the plant survival rate.

From the approaches to improving the current DLG testing framework, a methodology for testing precision planters in field was derived and tested in this study. Using a UAV with an RGB sensor, maize seeds planted by a precision planter with an open furrow could be semi-automatically segmented and georeferenced. The study established that high compaction of silty-clayey soil in sufficient width and with a uniform soil surface can ensure a visibility of maize seeds of > 90% when manually inspecting the orthomosaic. For the establishment of this methodology as the basis for a future testing framework for precision planters, it is expected that further testing of reconsolidation measures will contribute to an even higher rate of visible maize seeds. The increase in driving speed of the precision planter from 8 to 12 km/h showed no adverse effects on the visibility rate in this study at high reconsolidation. This finding suggests that this methodology may be suitable for practical driving speeds when testing precision planters with a catcher roller, such as the Precea 4500-2CC Super model. Nevertheless, subsequent studies should concentrate on soil reconsolidation and extend the investigation to higher driving speeds, as well as the applicability of this methodology to alternative precision planting systems.

The developed segmentation algorithm enabled the semi-automated segmentation of the maize seeds, with a recall of ≥ 0.96 and a precision of ≥ 0.62, by applying the Otsu threshold value to the a*-scale of the CIELab colour space and subsequent filtering by area size. However, this is only applicable when the lighting conditions are uniform due to overcast weather, and when there is a minimum distance of two centimetres between the seeds. While the sensitivity can be regarded as adequate in these instances, the accuracy must be enhanced. The implementation of alternative thresholding methods and additional filter algorithms could lead to further enhancements. The robustness of the algorithm for double placements with distances between maize seeds of less than two centimetres may also be optimised in this manner. In comparison to other approaches for plant position detection by UAV, the developed method has the advantage that it does not require a specific growth time window to be met. The experimental setup and data acquisition in the testing procedure can be completed within a day, which means improved planning flexibility according to current weather conditions. Additionally, with regard to the correct, georeferenced mapping of seed placement coordinates, further advantages over plant-based mapping were found: The calculation of coordinates is more straightforward, no assumptions about the average height of the plants are required, and with an $RMSE_{xy}$ between 1.7 and 5.1 mm, the mapping is more accurate than comparable works on plant-based mapping. However, it should be noted that the rolling of maize seeds on strongly reconsolidated soil may differ from rolling due to closure of the furrow with soil. This is an area that requires further research.

Overall, there is a high potential for updating the current testing framework for precision planters in field operations with maize by georeferenced mapping of maize seeds using RGB sensors carried by a UAV, in order to be able to test new technical functions of the machines. The subject of further development of this method should also be the transferability to crops with smaller and differently coloured seeds.

References

ASPRS Map Accuracy Standards Working Group (2015): ASPRS Positional Accuracy Standards for Digital Geospatial Data. Photogrammetric Engineering & Remote Sensing 81(3), pp. 1–26, https://doi.org/10.14358/PERS.81.3.A1-A26

Assefa, Y.; Vara Prasad, P.V.; Carter, P.; Hinds, M.; Bhalla, G.; Schon, R.; Jeschke, M.; Paszkiewicz, S.; Ciampitti, I.A. (2016): Yield Responses to Planting Density for US Modern Corn Hybrids: A Synthesis-Analysis. Crop Science 56(5), pp. 2802–2817, https://doi.org/10.2135/cropsci2016.04.0215

Bouten, M.; Meinel, T.; Kath-Petersen, W. (2019): Untersuchung des Einflusses einer diskontinuierlichen Ablage der P-Unterfußdüngung bei Mais – erste einjährige Ergebnisse von Feldversuchen. Landtechnik 74(1/2), S. 25–35, https://doi.org/10.15150/lt.2019.3202

Bozdoğan, A.M. (2008): Seeding uniformity for vacuum precision seeders. Scientia Agricola 65(3), pp. 318–322, https://doi.org/10.1590/S0103-90162008000300013

Budde, M.B. (2016): Erfassung und Bewertung der Einzelung von Feinstsämereien in Einzelkornsägeräten. Dissertation, Universität Bonn

Bullock, D.G.; Nielsen, R.L.; Nyquist, W.E. (1988): A Growth Analysis Comparison of Corn Grown in Conventional and Equidistant Plant Spacing. Crop Science 28(2), pp. 254–258, https://doi.org/10.2135/cropsci1988.0011183X002800020015x

Commission internationale de l'eclairage (CIE) (2007): Colorimetry. Understanding the CIE system, Vienna, Austria, https://doi.org/10.25039/TR.015.2018

Csurka, G.; Larlus, D.; Perronnin, F. (2013): What is a good evaluation measure for semantic segmentation? In: Procedings of the British Machine Vision Conference 2013, Ed. BMVA Press

Deutsche Landwirtschafts-Gesellschaft e.V. (DLG) (1991): DLG-Prüfrahmen für Einzelkornsägeräte. Groß-Umstadt

Duncan, W.G. (1984): A Theory to Explain the Relationship Between Corn Population and Grain Yield 1. Crop Science 24(6), pp. 1141–1145, https://doi.org/10.2135/cropsci1984.0011183X002400060032x

García-Martínez, H.; Flores-Magdaleno, H.; Khalil-Gardezi, A.; Ascencio-Hernández, R.; Tijerina-Chávez, L.; Vázquez-Peña, M.A.; Mancilla-Villa, O.R. (2020): Digital Count of Corn Plants Using Images Taken by Unmanned Aerial Vehicles and Cross Correlation of Templates. Agronomy 10(4), p. 469, https://doi.org/10.3390/agronomy10040469

Gnädinger, F.; Schmidhalter, U. (2017): Digital Counts of Maize Plants by Unmanned Aerial Vehicles (UAVs). Remote Sensing 9(6), p. 544, https://doi.org/10.3390/rs9060544

Golzarian, M.R.; Lee, M.-K.; Desbiolles, J.M.A. (2012): Evaluation of Color Indices for Improved Segmentation of Plant Images. Transactions of the ASABE 55(1), pp. 261–273, https://doi.org/10.13031/2013.41236

Götz, S.; Bernhardt, H. (2010): Produktionsvergleich von Gleichstandsaat und Normalsaat bei Silomais. Landtechnik 65(2), S. 107–110, https://doi.org/10.15150/lt.2010.604

Griepentrog, H.W. (1999): Zur Bewertung der Flächenverteilung von Saatgut. Agrartechnische Forschung 5(3), S. 117–124

Griepentrog, H.W.; Nrremark, M.; Nielsen, H.; Blackmore, B.S. (2005): Seed Mapping of Sugar Beet. Precision Agriculture 6(2), pp. 157–165, https://doi.org/10.1007/s11119-005-1032-5

Hengl, T. (2006): Finding the right pixel size. Computers & Geosciences 32(9), pp. 1283–1298, https://doi.org/10.1016/j.cageo.2005.11.008

Hernández-Hernández, J.L.; García-Mateos, G.; González-Esquiva, J.M.; Escarabajal-Henarejos, D.; Ruiz-Canales, A.; Molina-Martínez, J.M. (2016): Optimal color space selection method for plant/soil segmentation in agriculture. Computers and Electronics in Agriculture 122, pp. 124–132, https://doi.org/10.1016/j.compag.2016.01.020

Hoff, D.J.; Mederski, H.J. (1960): Effect of Equidistant Corn Plant Spacing on Yield. Agronomy Journal 52(5), pp. 295–297, https://doi.org/10.2134/agronj1960.00021962005200050019x

International Organization for Standardization (ISO) (1984): ISO 7256-1:1984 Sowing equipment — Test methods, Part 1: Single seed drills (precision drills), https://www.iso.org/standard/13910.html, accessed on 22 Jan 2024

Kachman, S.D.; Smith, J.A. (1995): Alternative Measures of Accuracy in Plant Spacing for Planters Using Single Seed Metering. Transactions of the ASAE 38(2), pp. 379–387, https://doi.org/10.13031/2013.27843

Landesamt für Bergbau, Energie und Geologie Niedersachsen (2023): Bodenkarte 1 : 50 000 (BK 50). https://www.lbeg.niedersachsen.de/karten_daten_publikationen/karten_daten/boden/bodenkarten/bodenkarte_150000/bodenkarte-1-50-000-bk50-655.html, accessed on 6 Dec 2023

Landini, G.; Randell, D.A.; Fouad, S.; Galton, A. (2017): Automatic thresholding from the gradients of region boundaries. Journal of Microscopy 265(2), pp. 185–195, https://doi.org/10.1111/jmi.12474

Mardanisamani, S.; Eramian, M. (2022): Segmentation of vegetation and microplots in aerial agriculture images: A survey. The Plant Phenome Journal 5(1), e20042, https://doi.org/10.1002/ppj2.20042

Midtiby, H.S.; Pastucha, E. (2022): Pumpkin Yield Estimation Using Images from a UAV. Agronomy 12(4), p. 964, https://doi.org/10.3390/agronomy12040964

National Aeronautics and Space Administration (NASA) (2019): What is Remote Sensing? https://www.earthdata.nasa.gov/learn/backgrounders/remote-sensing, accessed on 29 Jan 2024

Nielsen, R.L. (1993): Stand Establishment Variability in Corn. In: Proceedings of the 1993 Crop Production and Protection Conference, 12.02.1993, Iowa State University, Digital Press

Otsu, N. (1979): A Threshold Selection Method from Gray-Level Histograms. IEEE Transactions on Systems, Man, and Cybernetics 9(1), pp. 62–66, https://doi.org/10.1109/tsmc.1979.4310076

Panning, J.W.; Kocher, M.F.; Smith, J.A.; Kachman, S.D. (2000): Laboratory And Field Testing Of Seed Spacing Uniformity For Sugarbeet Planter. Applied Engineering in Agriculture 16(1), pp. 7–13, https://doi.org/10.13031/2013.4985

Pathak, H.; Igathinathane, C.; Zhang, Z.; Archer, D.; Hendrickson, J. (2022): A review of unmanned aerial vehicle-based methods for plant stand count evaluation in row crops. Computers and Electronics in Agriculture 198, S. 107064, https://doi.org/10.1016/j.compag.2022.107064

Riehle, D.; Reiser, D.; Griepentrog, H.W. (2020): Robust index-based semantic plant/background segmentation for RGB-images. Computers and Electronics in Agriculture 169, p 105201, https://doi.org/10.1016/j.compag.2019.105201

SaatV (2022): Saatgutverordnung in der Fassung der Bekanntmachung vom 8. Februar 2006 (BGBl. I S. 344), die zuletzt durch Artikel 1 der Verordnung vom 13. Juli 2022 (BGBl. I S. 1186) geändert worden ist

Sangoi, L. (2001): Understanding Plant Density Effects on Maize Growth and Development. An Important Issue to Maximize Grain Yield. Ciência Rural 31(1), pp. 159–168, https://doi.org/10.1590/S0103-84782001000100027

Schuchmann, G.H. (2019): DLG-Testmethoden und Entwicklungstrends im Bereich der Sätechnik. https://www.dlr-eifel.rlp.de/Internet/global/themen.nsf/341173a1418617d1c1256f49003f5306/2E89FDA5B65DBC97C1258399003BB5D1/$FILE/Georg%20Horst%20Schumann%20-%20DLG-Testmethoden%20und%20Entwicklungstrends%20im%20Bereich%20der%20S%C3%A4technik%20(AT2%20017).pdf, accessed on 29 Jan 2024

Shuai, G.; Martinez-Feria, R.A.; Zhang, J.; Li, S.; Price, R.; Basso, B. (2019): Capturing Maize Stand Heterogeneity Across Yield-Stability Zones Using Unmanned Aerial Vehicles (UAV). Sensors 19(20), p. 4446, https://doi.org/10.3390/s19204446

Thorp, K.R.; Steward, B.L.; Kaleita, A.L.; Batchelor, W.D. (2007): Using Aerial Hyperspectral Remote Sensing Imagery to Estimate Corn Plant Stand Density. Transactions of the ASABE 51(1), pp. 311–320, https://doi.org/10.13031/2013.24207

Voit, B.; Schnellhammer, R.; Eder, J.; Killermann, B. (2010): Einfluss von Keimfähigkeit und Triebkraft auf den Feldaufgang und Ertrag bei Mais. In: Züchtung und Genressourcen gegen abiotische Stressfaktoren, markergestützte Selektion in der Praxis. 60. Tagung, 24.–26. November 2009, Irdning, Lehr- und Forschungsanstalt für Landwirtschaft Raumberg-Gumpenstein, S. 125–128

Vong, C.N.; Conway, L.S.; Zhou, J.; Kitchen, N.R.; Sudduth, K.A. (2021): Early corn stand count of different cropping systems using UAV-imagery and deep learning. Computers and Electronics in Agriculture 186, p. 106214, https://doi.org/10.1016/j.compag.2021.106214

Wang, Y.; Lv, H.; Deng, R.; Zhuang, S. (2020): A Comprehensive Survey of Optical Remote Sensing Image Segmentation Methods. Canadian Journal of Remote Sensing 46(5), pp. 501–531, https://doi.org/10.1080/07038992.2020.1805729

Woli, K.P.; Burras, C.L.; Abendroth, L.J.; Elmore, R.W. (2014): Optimizing Corn Seeding Rates Using a Field's Corn Suitability Rating. Agronomy Journal 106(4), pp. 1523–1532, https://doi.org/10.2134/agronj14.0054

Zhang, J.; Basso, B.; Price, R.F.; Putman, G.; Shuai, G. (2018): Estimating plant distance in maize using Unmanned Aerial Vehicle (UAV). PLoS ONE 13(4), e0195223, https://doi.org/10.1371/journal.pone.0195223

Authors

Steffen Konnemann, M.Sc., and **Eike Hunze, M.Sc.**, were research associates, **Prof. Dr.-Ing. Frank Beneke** is the head of the Section of Agricultural Engineering at the Georg-August-Universität of Göttingen, Gutenbergstr. 33, 37075 Göttingen, Deutschland. E-mail: steffen.konnemann@uni-goettingen.de

Notes and Acknowledgements

We would like to express our gratitude to Mr. **Georg Horst Schuchmann**, Test engineer at the DLG Competence Center Agriculture, for providing information on the currently used DLG testing framework for precision planters and for his critical evaluation of the results in terms of their applicability to practical use.

The project is supported by funds of the Federal Ministry of Food and Agriculture (BMEL) based on a decision of the Parliament of the Federal Republic of Germany via the Federal Office for Agriculture and Food (BLE) under the innovation support programme (Project number: 28DE104A18).